Theory of light-beam propagation at nonlinear interfaces. II. Multiple-particle and multiple-interface extensions

A. B. Aceves, J. V. Moloney,* and A. C. Newell
Department of Mathematics, University of Arizona, Tucson, Arizona 85721
(Received 11 August 1988)

The theory presented in the preceding paper is extended to account for incident optical beam breakup into multiple self-focused channels and to deal with multiple reflection and transmission at multiple interfaces. Beam breakup is explained by examining the decomposition of the channel in one medium, into its soliton and radiation components after it has crossed into the new medium. A formula is derived which gives the criterion for the number of channels appearing as a consequence of breakup. This formula also provides analytic expressions for the individual self-focused channel powers and the amount of radiation generated. An important observation here is that the amount of radiation generated at the interface shrinks rapidly as a function of increasing channel number N. Each new component generated can be treated as a separate equivalent particle moving in its own equivalent potential. The theory of the preceding paper [Aceves, Moloney, and Newell, Phys. Rev. A **39**, 1809 (1989)] can therefore be applied directly to show that low-power channels generated in the breakup will suffer reflection while higher-power channels will undergo transmission. An added ingredient to allow for mutual-channel interaction is the soliton-collision formula. The multiple-interface extension of the single-interface problem results from patching individual single-interface equivalent potentials together. The theory is illustrated with two applications: (i) a nonlinear version of a directional coupler requiring just two interfaces and (ii) trapping of a channel at an interface by a ramped linear refractive index.

I. INTRODUCTION

The equivalent-particle theory presented in the preceding paper,[1] hereafter labeled paper I, is only valid in the nonlinear regime when the nonlinear optical coefficient ratio $\alpha=\alpha_0/\alpha_1$ is greater than $\frac{4}{9}$. There we established that the equivalent-particle theory was valid in a wide region of physical parameter space. The study in the present paper is confined to this fully nonlinear regime. As the nonlinear optical coefficient in the right-hand medium increases, the larger self-focusing nonlinearity leads to breakup of the incident channel into multiple channels after its peak has crossed the interface. This breakup should be contrasted with the phenomenon of partial transmission and reflection well known in the linear and confined to the hornlike intermediate regimes, as discussed in paper I. In the linear case, this latter phenomenon is associated with the Fourier decomposition of the linear wave packet and subsequent trajectories of individual Fourier plane-wave components spanning the critical angle for total internal reflection. In the intermediate nonlinear regime, the interface, as a perturbation, excites other nonlinear modes or radiation leading to a splitting of the incident wave packet. The behavior to be described below lies in a region of parameter space remote from the latter linear or intermediate regimes. The asymptotic behavior of each new channel will now depend on its individual power, being reflected if $v_0^2/2 < U(\infty)$ (see paper I) or transmitted if $v_0^2/2 > U(\infty)$. This breakup behavior will be quantitatively explained in Sec. II by considering the incident channel at the interface as the initial data for evolution under the nonlinear Schrödinger (NLS) equation appropriate to the new medium, using results developed in Ref. 2. In effect, we find that the incident channel behaves as an N-soliton bound state for the new medium. The interface acting as localized perturbation on this bound state, lifts the degeneracy of its eigenvalue, splitting the N-soliton wave packet into N individual propagating components. Each component is now a soliton solution in the new nonlinear medium and its subsequent asymptotic behavior can be read off from its associated equivalent potential or phase portrait. Experimental evidence for such beam breakup has already been obtained,[3] following observations of such behavior in an earlier numerical study of a Gaussian beam incident at an angle close to critical at a linear-nonlinear interface.[4] This optical beam breakup is insensitive to the specific shape of the initial data, so our theory presented here, which for convenience adopts a sech-like initial profile, provides a quantitative description of the phenomenon.

The equivalent-particle theory valid for $\frac{4}{9} \le \alpha < 1$, is extended to multiple interfaces in Sec. III, by patching together individual equivalent-particle potentials in order to construct a global composite potential. Our only assumption is that the characteristic self-focused channel width is narrower than or comparable to the individual interface separations. Two cases will be considered. In one the interface separation is much larger than the self-focused channel width and the single-interface theory applies with minor modifications. The second case involving interface separations comparable to the channel

width is the thin-film waveguide limit and introduces an additional important scaling parameter, namely, ηd, where η is proportional to the power in the channel and d is the thin-film width. In this latter case we recover the nonlinear waveguide picture including global bifurcation features[5] and stability.[6,7]

Two applications presented in Sec. IV highlight the very special properties of solitons, namely, their particle-like properties and resistance to perturbations. We demonstrate how an end-fire coupled channel, propagating as a stable trapped nonlinear surface wave along the interface, can be switched to a neighboring interface by an additional channel incident at an angle close to critical for total internal reflection. This switching action exploits the elastic particle-collision properties of solitons. Trapping at an interface is achieved by a linearly ramped refractive index, which acts as a decelerating force on the particle. Section V illustrates briefly how an $N=2$ soliton wave packet splits due to the effect of the perturbation by an interface.

II. BEAM BREAKUP INTO MULTIPLE SELF-FOCUSED CHANNELS

This section is devoted to a study of incident channel breakup in the new medium. The relevant equations from I are reproduced here for convenience. The scaled transverse electric (TE) field amplitude $A(x,\tau)$ obeys the following perturbed NLS equation:

$$i\frac{\partial A}{\partial \tau}+\frac{\partial^2 A}{\partial x^2}+2|A|^2A=VA\ , \tag{1}$$

where, in terms of the original unscaled variables, we have

$$F(x,z)=\sqrt{2/\alpha_0}\,A(x,\tau)\exp[i(\beta^2-n_0^2)z]$$

and $2\beta\tau=z$. The perturbation potential $V(\bar{x})$ is given by

$$V(\bar{x})=\begin{cases}-\Delta-2(\alpha^{-1}-1)|A|^2, & x<0\\ 0, & x>0.\end{cases}$$

The asymptotic behavior of a wave packet with a soliton shape in the left-hand medium as it crosses the interface into the right-hand medium will now be investigated. In particular, we wish to know whether it remains as a single entity or breaks up into multiple self-focused channels in the new medium. We also wish to measure the amount of radiation (nonsoliton components) generated as a consequence of the interaction with the interface. A general initial-value problem of this sort was studied originally in a classic paper by Satsuma and Yajima.[2] Here we adapt their results to our specific problem. Details of the soliton analysis are given in the Appendix. The main results are noted here.

If the wave packet with modulus

$$|F(x,z)|=\sqrt{2/\alpha_0}\,2\eta_0\,\mathrm{sech}[2\eta_0(x-\bar{x})]$$

crosses the interface from left to right and if the speed of the equivalent particle at the time it crosses the interface is v, it will decompose into a sequence of N solitons with

$$\frac{1}{\sqrt{\alpha}}-\frac{1}{2}<N\le\frac{1}{\sqrt{\alpha}}+\frac{1}{2} \tag{2}$$

and radiation. Observe that the number of new soliton wave packets increases as the nonlinear refractive index of the right-hand medium, α_1, increases. The initial velocity of each of the new solitons is also v but the amplitudes are given by

$$\eta_{1r}=2\eta_0\left[\frac{1}{\sqrt{\alpha}}-r+\frac{1}{2}\right],\quad r=1,\ldots,N\ . \tag{3}$$

The amount of radiation can be calculated using the trace formula (see Appendix)

$$\int_{-\infty}^{\infty}AA^*dx=4\sum_{r=1}^{N}\eta_{1r}-\frac{2}{\pi}\int_0^{\infty}\ln(1-|R|^2)d\varsigma\ , \tag{4}$$

where $R(\varsigma)$ is the reflection coefficient obtained from the scattering data of the linear eigenvalue problem (A1). It measures the amount of radiation in the mode ς. In the limit of small $|R(\varsigma)|$, $-\ln(1-|R|^2)\sim|R|^2$, and in the absence of soliton components, (4) is simply Parseval's identity.

Since the total power $P=\int_{-\infty}^{\infty}FF^*dx=8\eta_0/\alpha_0$ is conserved, we have that

$$\frac{8\eta_0}{\alpha_0}=\frac{8}{\alpha_1}\sum_{r=1}^{N}\eta_{1r}-\frac{4}{\alpha_1\pi}\int_0^{\infty}\ln(1-|R|^2)d\varsigma\ .$$

The difference between $8\eta_0/\alpha_0$ and $(8/\alpha_1)\sum_{k=1}^{N}\eta_{1r}$ is the amount converted into radiation. From Eq. (3), this difference is equal to $8\eta_0/\alpha_0(1-N\sqrt{\alpha})^2$. Observe then that if $\frac{4}{45}<\alpha\le\frac{4}{9}$, $N=2$ and at most 4% of the incident power goes into radiation; if $\frac{4}{49}<\alpha\le\frac{4}{25}$, $N=3$ and at most 2% goes into radiation, and for large N it is at most $1/(2N+1)^2$ of the power in the incident beam. Also observe that, as α tends to 1, the amount of radiation produced is negligible as we are in the strongly nonlinear regime (see Sec. III of paper I). In fact, if $\alpha>\frac{4}{9}$, then $N=1$ and $\eta_1=2\eta_0(1/\sqrt{\alpha}-\frac{1}{2})$. Now the amount of power $P_T=8\eta_1/\alpha_1$ carried by the new wave packet in the right-hand medium is $(2\sqrt{\alpha}-\alpha)P_I$, where $P_I=8\eta_0/\alpha_0$ is the power of the original wave packet. This means that the amount of power converted into radiation is

$$\frac{4}{\alpha_1\pi}\int_0^{\infty}\ln(1-|R|^2)d\varsigma=(1-\sqrt{\alpha})^2\frac{8\eta_0}{\alpha_0}\ .$$

For the worst possible case $\alpha=\frac{4}{9}$, $(1-\sqrt{\alpha})^2\sim0.11$; therefore, in all cases the $N=1$, the amount of power lost into radiation is less than 11% and goes to zero as α tends to 1.

In the new medium, a single wave packet will propagate as an equivalent particle in a potential defined by the material properties and its own power. However, if a bound state of N solitons is produced, the problem becomes one of N interacting particles in a composite potential. Eventually the bound state is broken into N individual packets, each traveling in its own effective potential. When the breakup occurs depends on the velocity of the equivalent particle at the interface. The smaller the

velocity, the sooner the breakup will occur, and in most cases studied here with the initial velocity always of the order of $\sqrt{\Delta}$, breakup always occurs immediately after crossing the interface. In particular, the packets with the smaller amplitudes will have higher S values and this may very well mean that they will reflect back into the left-hand medium. The N-particle theory will not be carried out in this work.

At this point we present some data which support the accuracy of our decomposition computation. Table I compares the predicted and observed values of η_{1r}. The agreement is very good. Figure 1 shows two cases of a single wave packet decomposing into multisoliton components in the right-hand medium. In the first case two sizeable wave packets are transmitted to, and remain in, the right-hand medium and one very small one is reflected. Since the latter does not have enough power to create a soliton wave packet in the left-hand medium when it recrosses the interface, it eventually disperses as radiation and decays. In the second case, the angle of incidence of the incoming wave packet is big enough to guarantee that all three transmitted wave packets remain in the right-hand medium.

When a wave packet which has a perfect soliton shape for the right-hand medium crosses to the left, the number of wave packets N lies between $\sqrt{\alpha}-\frac{1}{2}$ and $\sqrt{\alpha}+\frac{1}{2}$. Since $\alpha \leq 1$, this means that a wave packet entering from the right will decompose into at most one soliton whose initial velocity is v and whose amplitude η_0 is $2\eta_1(\sqrt{\alpha}-\frac{1}{2})$. Again note that as $\alpha \to 1$, $\eta_0 \to \eta_1$. The trace formula now gives

$$\frac{8\eta_1}{\alpha_1} = H(\sqrt{\alpha}-\tfrac{1}{2})\frac{8\eta_0}{\alpha_0} - \frac{4}{\alpha_0 \pi}\int_0^\infty \ln(1-|R|^2)d\varsigma \ ,$$

where H is the Heaviside function. For $\alpha > \frac{1}{4}$, the amount of radiation created is proportional to $(1-\sqrt{\alpha})^2/\alpha$, which is again small for α close to unity. In Fig. 2, we show a situation in which $\alpha = \frac{1}{4}$, which as we said above, is too small to create a soliton packet in the left-hand medium. The packet of radiation which is created disperses and decays.

Although the dynamics is more complicated when there is a large nonlinear refractive-index mismatch, one can carry out the decomposition calculation of each packet as it crosses the interface and follow the dynamics of the different components. However, care has to be taken because the different new components can interact with each other and produce phase shifts, a property we will describe and exploit for application purposes in Sec. IV. Nevertheless, in principle, the total dynamics can be reconstructed by piecing together the trajectories of each wave packet.

TABLE I. Comparison between the predicted values of the amplitudes (η_i) of the solitons that are created after breakup in the right-hand media, with the obtained values computed from the numerical integration of (1.1), for different initial velocities (angles of incidence). The blank spaces indicate that we were not able to numerically determine the values of the amplitudes of those solitons.

α	Normalized power of initial wave packet	Theoretical η_i's of transmitted wave packets	Numerical η_i's of transmitted wave packets for three different initial velocities. Initial velocity 0.40	0.20	0.160
0.125	2	$\eta_1=0.292$ $\eta_2=0.166$ $\eta_3=0.038$	0.33	0.313	
	4	$\eta_1=0.584$ $\eta_2=0.332$ $\eta_3=0.076$	0.50 0.33	0.46 0.30	
0.25	2	$\eta_1=0.375$ $\eta_2=0.125$	0.38	0.372	0.373
	4	$\eta_1=0.750$ $\eta_2=0.250$	0.65 0.26	0.630	
0.375	2	$\eta_1=0.425$ $\eta_2=0.050$	0.442	0.435	0.410
	4	$\eta_1=0.850$ $\eta_2=0.100$	0.790	0.770	
0.5	2	$\eta_1=0.457$	0.460	0.464	0.46
	4	$\eta_1=0.914$	0.860	0.870	
0.625	2	$\eta_1=0.482$	0.483	0.483	0.496
	4	$\eta_1=0.964$	0.93	0.93	

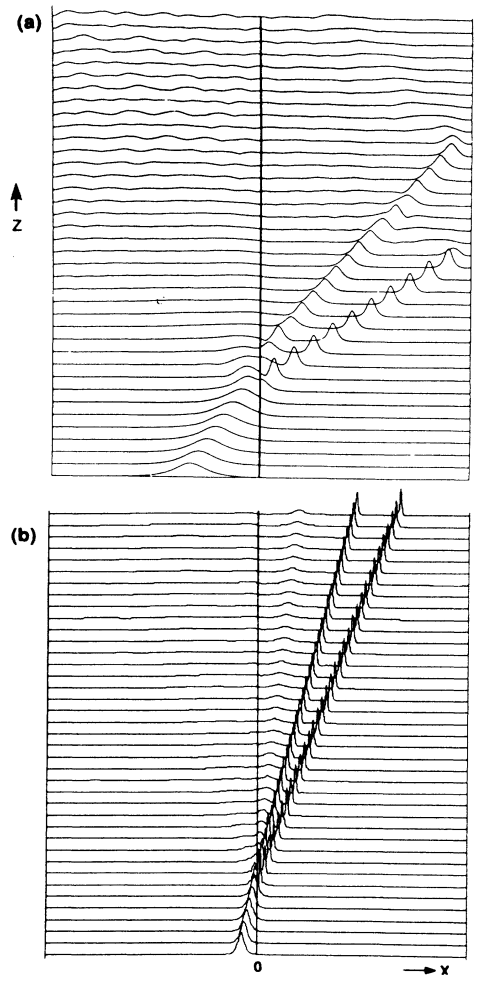

FIG. 1. Soliton breakup in the right-hand medium. In (a) an incoming wave packet breaks into three as it crosses the interface, with the smallest one being reflected back to the left-hand medium where it eventually disperses into radiation. In (b) the angle of incidence is bigger, so that no wave packet is reflected. In both cases, the amplitudes of each soliton are very close to the theoretical predictions. Here $P=4$, $v_0=0.4$ in (a) and 1.0 in (b); $\Delta=0.1$ and $\alpha=0.125$.

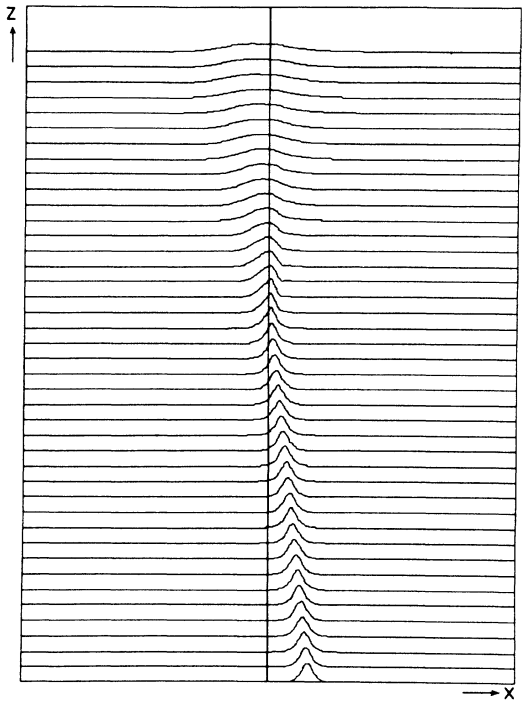

FIG. 2. Evolution of a wave packet that initially is in the right-hand medium and, once it crosses the interface, it loses its soliton shape, becoming a dispersive wave as predicted by the theory. The parameters are the same of that of the previous figure, except that the wave packet is initially in the right-hand medium and $v_0=-1.0$.

III. MULTIPLE INTERFACES

Consider a geometry for a waveguide where three different media are separated by two interfaces at $x=x_1$ and $x=x_2$. The refractive indexes in the various media are given by

$$n^2(x,|F|^2)=n_j^2+\alpha_j|F|^2, \quad j=1,2,3$$

where we only consider the case in which the ratio of smaller to bigger α_j on two neighboring materials is always bigger than $\frac{4}{9}$, so that a single wave packet prevails in all media. These refractive indexes appear as coefficients in the original unscaled nonlinear partial differential equation (1) of paper I.

To construct the equivalent potential we proceed as in I by assuming first that a wave packet propagates in one medium, say medium 2, and does not cross any interface. We define the field F to be of the form

$$F(x,z)=\sqrt{2}/\alpha_2 A(x,\tau)e^{i(\beta^2-n_2^2)z},$$

then $A(x,\tau)$ satisfies Eq. (1), where now V is

$$V(x)=\begin{cases}\Delta_2^{(1)}-2(\alpha_{12}-1)|A|^2, & x_0<x<x_1\\ 0, & x_1<x<x_2\\ \Delta_2^{(3)}-2(\alpha_{32}-1)|A|^2, & x_2<x<x_4\end{cases}$$

where $\Delta_2^{(j)}=n_2^2-n_j^2$, $\alpha_{j2}=\alpha_j/\alpha_2$, $x_0=-\infty$, and $x_4=\infty$.

In (1) we use for A a soliton form and, following the steps of Sec. IV in paper I, the new effective potential for and equivalent-particle dynamics of a wave packet traveling in medium 2 is

$$U_2(\bar{x})=-\Delta_2^{(1)}\left[1-\frac{1}{S_2^{(1)}}\right]\tanh[2\eta_2(\bar{x}-x_1)]$$
$$-\frac{\Delta_2^{(1)}}{3S_2^{(1)}}\tanh^3[2\eta_2(\bar{x}-x_1)]$$
$$+\Delta_2^{(3)}\left[1-\frac{1}{S_2^{(3)}}\right]\tanh[2\eta_2(\bar{x}-x_2)]$$
$$+\frac{\Delta_2^{(3)}}{3S_2^{(2)}}\tanh^3[2\eta_2(\bar{x}-x_2)]+C_2\ , \qquad (5)$$

where $S_2^{(j)}=\Delta_2^{(j)}\alpha_2/4(\alpha_j-\alpha_2)\eta_2^2$, $\eta_2=\alpha_2 P^2/8$, and P the total power.

If all the nonlinear mismatches are close to 1, we neglect radiation as we did in the case of the single interface, and write a composite potential to describe the global dynamics of a wave packet propagating in such a waveguide,

$$U(\bar{x})=[1-H(\bar{x}-x_1)]U_1(\bar{x})$$
$$+[H(\bar{x}-x_1)-H(\bar{x}-x_2)]$$
$$\times U_2(\bar{x})+H(\bar{x}-x_2)U_3(\bar{x})\ ,$$

where H is the Heaviside function,

$$U_j(\bar{x})=\sum_{\substack{l=1\\ l\neq j}}^{3}\left[\Delta_j^{(l)}\left[1-\frac{1}{S_j^{(l)}}\right]\{\tanh[2\eta_j(\bar{x}-x_{l-1})]\right.$$
$$-\tanh[2\eta_j(\bar{x}-x_l)]\}$$
$$+\frac{\Delta_j^{(l)}}{3S_j^{(l)}}\{\tanh^3[2\eta_j(\bar{x}-x_{l-1})]$$
$$\left.-\tanh^3[2\eta_j(\bar{x}-x_l)]\}+C_j\right] \qquad (6)$$

and $\Delta_j^{(l)}=n_j^2-n_l^2$, $\eta_j=\alpha_j P/8$, $S_j^{(l)}=\Delta_j^{(l)}\alpha_j/4(\alpha_j-\alpha_l)\eta_j^2$. We choose the constant C_j in (6) so that $U(\bar{x})$ is continuous at each interface.

In general, if we have N interfaces located at x_j, $j=0,1,2,\ldots,N+1$ with $x_0=-\infty$, and $x_{N+1}=\infty$, the composite potential is

$$U(\bar{x})=\sum_{j=1}^{N+1}[H(\bar{x}-x_{j-1})-H(\bar{x}-x_j)]U_j(\bar{x})\ , \qquad (7)$$

where $U_j(\bar{x})$ is as in (6) where now l runs from 1 to $N+1$, omitting $l=j$.

We now consider two cases involving multiple interfaces. First, we have that if the wave packet width is small compared to the distance between interfaces, then if the wave packet is close to one interface, say, x_j, the equivalent potential is of the form

$$U(\bar{x})\sim[1-H(\bar{x}-x_j)]\left[\Delta_j^{(j+1)}\left[1-\frac{1}{S_j^{(j+1)}}\right]\tanh[2\eta_j(\bar{x}-x_j)]+\frac{\Delta_j^{(j+1)}}{3S_j^{(j+1)}}\tanh^3[2\eta_j(\bar{x}-x_j)]\right]$$
$$+H(\bar{x}-x_j)\left[-\Delta_{j+1}^{(j)}\left[1-\frac{1}{S_{j+1}^{(j)}}\right]\tanh[2\eta_{j+1}(\bar{x}-x_j)]-\frac{\Delta_{j+1}^{(j)}}{3S_{j+1}^{(j)}}\tanh^3[2\eta_{j+1}(\bar{x}-x_j)]\right]+G(\bar{x})\ , \qquad (8)$$

where $G(\bar{x})$ accounts for the contributions from (6) not included in (7), all of which are slowly varying functions of $\bar{x}$ or, in other words, $|dG/d\bar{x}|\ll 1$. This is true because when the wave packet is narrow and propagating in the neighborhood of a particular interface, other interfaces, in effect, do not perturb its evolution. In terms of the equivalent particle, what we are saying is that the local potential in the neighborhood of an interface is like that of the single-interface case; thus the composite potential can be constructed for this particular case by simply "patching" potentials like that of Fig. 12 of paper I.

In Figs. 3 and 4, we examine two situations, each with three interfaces, and in both cases there are three minima in $U(\bar{x})$ corresponding to three stable stationary solutions. We confirmed the existence of these solutions by numerically integrating the full equation, with wave packets centered at the location of the local minima used as initial conditions. Figure 5 shows one of these solutions when the potential is as shown in Fig. 3. The exact form of the stationary solutions for this case are also sech-like solutions in each medium with the particular parameters obtained from the continuity conditions.

One can also expect that in this approximation, if we put two equivalent particles, each in a different well of the composite potential, they will not interaction with each other and remain in their original positions. Figure 6 shows one such case where two narrow wave packets propagate undisturbed, each near a minimum of the equivalent potential. Although we did not consider other cases with three or more packets, the same should be true. In fact, we have found new multipeak stable stationary wave packets in a multiple-interface waveguide by simply locating each peak at the minimum of a composite potential. These are the fully nonlinear generalizations of the well-known supermode solutions in multiple layered linear waveguides.[8]

The approximation used above fails when the distance between interfaces becomes of the same order as the width of the wave packet. This we call the thin-film waveguide limit. We present here as an example, a symmetric waveguide with two interfaces, one at $x=-x_1$ and the other at $x=x_1$. For $x<-x_1$ and $x>x_1$, the nonlinear index of refraction is $n^2=n_1^2+\alpha_1^2|F|^2$, whereas for the dielectric between the two interfaces n^2 is

$n_0^2+\alpha_0|F|^2$. We will only consider the case $n_0^2>n_1^2$, $\alpha_0<\alpha_1$, since any other combination could be studied in a similar way. Also we only consider narrow wave packets and $\alpha_0/\alpha_1>\frac{4}{9}$, so that again we neglect radiation. This problem is similar to the thin-film waveguide where $\alpha_0=0$, which has been studied in some detail earlier.[5,6,9] In order to characterize the different behavior of the composite potential, a new parameter will be introduced; it is $\eta_0 d$, where $d=2x_1$ is the distance between the two interfaces. We will now show how $U(\bar{x})$ behaves as a function of this parameter and in particular how the stability properties of the stationary surface waves change as $\eta_0 d$ changes; the nonlinear wave localized between the two interfaces could equally well be referred to as a non-

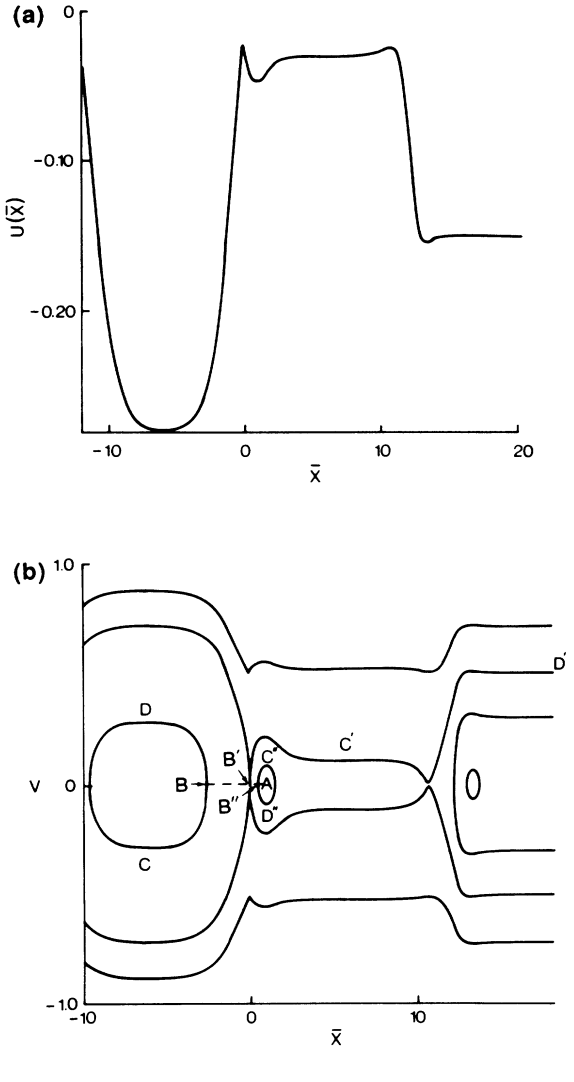

FIG. 3. Potential and phase plane for a nonlinear waveguide with three interfaces located at $x=-12$, 0, and 12. In (b) we show three typical trajectories of a wave packet initially propagating parallel to the second interface, after a second wave packet collides with it (see Fig. 8). In the first one, trajectory $ABCD$, the equivalent particle oscillates between the first and second interface. In the second one, $AB'C'D'$, the particle ends up at ∞, and in the third one, $AB''C''D''B''$, the particle oscillates about the center to the right near the second interface. Here $n_1^2=n_3^2=0.13$, $n_2^2=0.23$, $n_4^2=0.01$, and $\alpha_1=\alpha_3=2.0$, $\alpha_2=1.5$, and $\alpha_4=2.5$. The power of the corresponding wave packet is $P=2$.

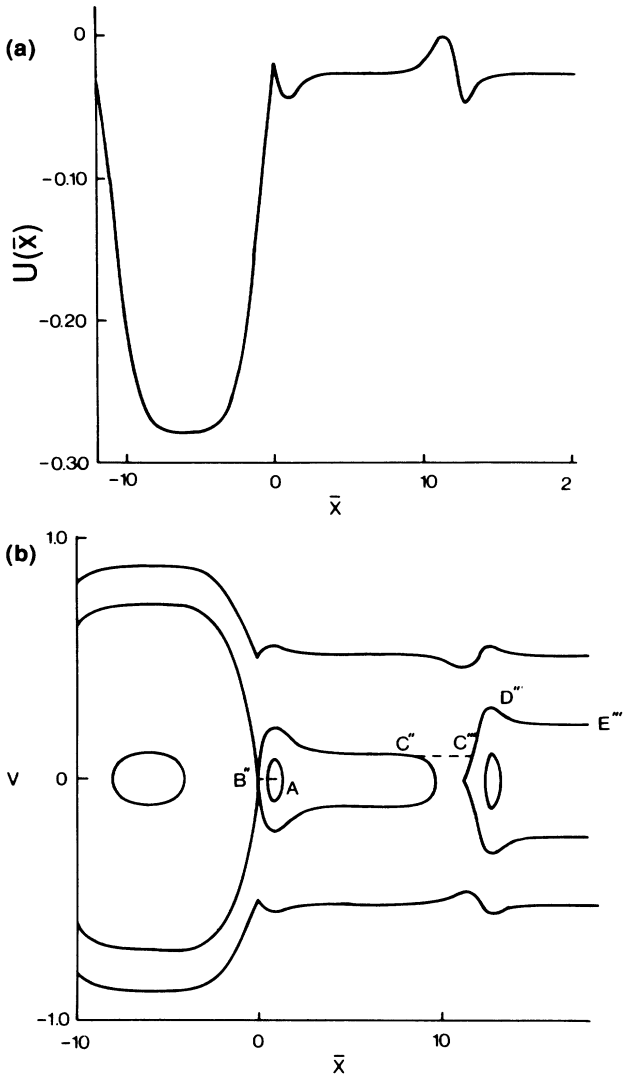

FIG. 4. Potential and phase plane for case study 2. The parameters of the media are the same as for Fig. 3, but the power of the corresponding wave packet is now $P=1.6$. Now the local maximum of U near the third interface is bigger than the local maximum near the second interface. In the phase plane we show again the trajectory of a packet initially propagating parallel to the second interface, after a second wave packet collides with it and shifts its position to B'' (see Fig. 9). After that, the particle starts moving to the right until it has another collision at C'', with the displacement now happening in opposite directions, and with the second particle ending up at $-\infty$.

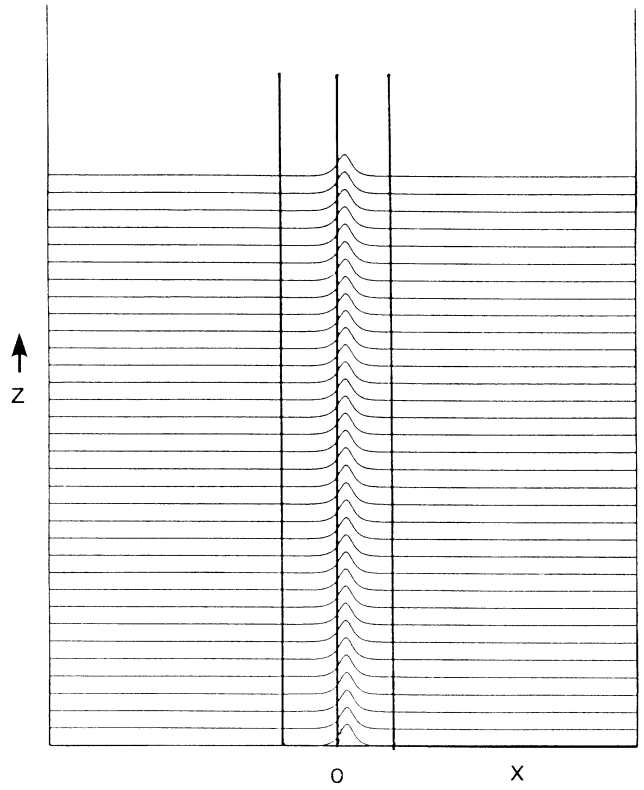

FIG. 5. Evolution of a wave packet propagating parallel to the second interface, where the equivalent potential has a minimum. As we can see, this wave packet is stable, as predicted by the theory. The power of the wave packet is $P=2.0$, and the parameters of the media are the same as those of Fig. 3.

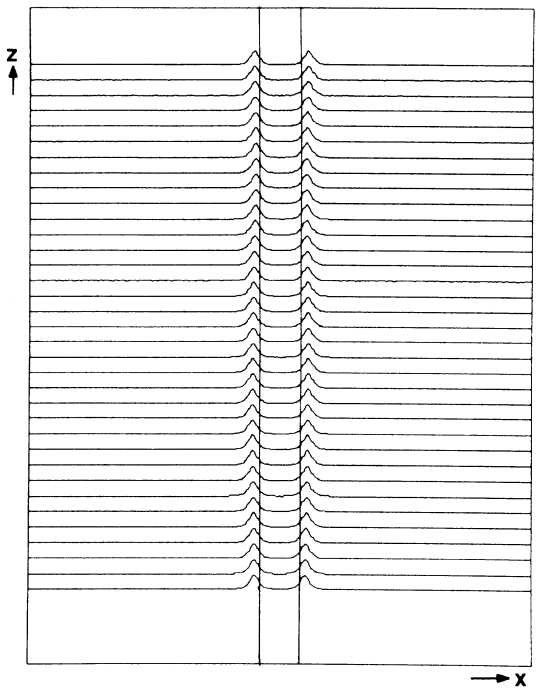

FIG. 6. Two narrow wave packets each propagating near and parallel to an interface. In the equivalent potential [see Fig. 7, regime (IV)], a minimum of U is located at the peak of each wave packet. The total power of the field is $P=4.0$, twice that of the single-peak wave packet of Fig. 5.

linear guided wave. The fact that we are considering a symmetric waveguide considerably simplifies the analysis. First, as one can expect, the composite potential is symmetric; therefore, we only need to look at its behavior for $\bar{x}\geq 0$ and it has a simpler form than the general case,

$$U_s(\bar{x})=[1-H(\bar{x}+x_1)+H(\bar{x}-x_1)]U_{s1}(\bar{x})$$
$$+[H(\bar{x}+x_1)-H(\bar{x}-x_1)]U_{s0}(\bar{x}) ,$$

where

$$U_{si}=\Delta_s\left[1-\frac{1}{S^{(i)}}\right]\{\tanh[2\eta_i(\bar{x}+x_1)]-\tanh[2\eta_i(\bar{x}-x_1)]\}+\frac{\Delta_s}{3S^{(i)}}\{\tanh^3[2\eta_i(\bar{x}+x_1)]-\tanh^3[2\eta_i(\bar{x}-x_1)]\}+C_i,\quad i=0,1$$

$\eta_i=\alpha_i P/8$, $S^{(i)}=\Delta_s\alpha_i/4(\alpha_0-\alpha_1)\eta_i^2$, and $\Delta_s=n_1^2-n_0^2$.

We observe first that from its symmetry properties, U_s must have a critical point at $\bar{x}=0$. Whether it is a maximum or a minimum depends on d^2U_s/dx^2. We have that

$$\frac{d^2U_s(\bar{x}=0)}{dx^2}=-8\eta_0\Delta_s\tanh(\eta_0 d)\operatorname{sech}^2(\eta_0 d)\left[1-\frac{2}{S^{(0)}}\operatorname{sech}^2(\eta_0 d)\right],$$

therefore $\bar{x}=0$ is a minimum (maximum) if $S^{(0)}\gtrless 2\operatorname{sech}^2\eta_0 d$.

For $0<\bar{x}<x_1$, there is at most one critical point of U_s (this result was confirmed numerically since we have no proof of it). Instead of explicitly finding it, when it exists, it is easier only to prove its existence by looking at the behavior of $dU_s/d\bar{x}$ at the interface x_1^-. After simplifications,

$$\frac{dU_s}{d\bar{x}} = -2\eta_0\Delta_s(1-\mathrm{sech}^2\eta_0 d)\left[1-\frac{1+\mathrm{sech}^2 2\eta_0 d}{S^{(0)}}\right],$$

therefore $dU_s/d\bar{x} \lesseqgtr 0$ if $S^{(0)} \gtreqless (1+\mathrm{sech}^2 2\eta_0 d)$. This result combined with the behavior of U_s at $\bar{x}=0$ gives as necessary conditions for having two symmetrical critical points inside the interfaces that $S^{(0)} > 1+\mathrm{sech}^2 2\eta_0 d$ and $S^{(0)} < 2\,\mathrm{sech}^2 2\eta_0 d$, then the critical points are minima; or that $S^{(0)} < 1+\mathrm{sech}^2 2\eta_0 d$ and $S^{(0)} > 2\,\mathrm{sech}^2\eta_0 d$ with the critical points being maxima.

The behavior of U_s in the outer media can be analyzed similarly. We have observed from numerical evaluations of U_s for different parameter values that again there is at most one critical value of U_s for $\bar{x} > x_1$. Since U_s is an increasing function of $\bar{x}$ as $\bar{x} \to \infty$, we will infer the existence of the critical point from the behavior of U_s at x_1^+. We have that

$$\frac{dU_s(x_1^+)}{d\bar{x}} = -2\eta_1\Delta_s[1-\mathrm{sech}^2(2\eta_1 d)] \times \left[1-\frac{1+\mathrm{sech}^2(2\eta_1 d)}{S^{(1)}}\right].$$

Using the fact that $\eta_1=(\alpha_1/\alpha_0)\eta_0$ and $S^{(1)}=(\alpha_1/\alpha_0)S^{(0)}$, the condition for existence of critical points in the outer media is

$$\frac{dU_s(x_1^+)}{d\bar{x}} < 0 \quad \text{or} \quad S^{(0)} < \frac{\alpha_0}{\alpha_1}\left[1+\mathrm{sech}^2\left[2\frac{\alpha_1}{\alpha_0}\eta_0 d\right]\right],$$

and they are always minima.

We show in Fig. 7 in an $S^{(0)},\eta_0 d$ plane all the regions of different potentials for fixed values of Δ_s and α_0/α_1. From here we can extract to a first approximation the existence and stability properties of surface and guided waves in such a configuration. Note that the scaling of our problem allows us to extract very general information regarding bifurcation of new branches and their stability under widely differing physical conditions. For example, keeping the power which is proportional to η_0 fixed, and reducing the thin-film waveguide width d corresponds to moving along a horizontal line at constant S_0; both α and the linear mismatch Δ are also fixed. For example, at $S_0=0.25$ as the guide width d reduces, the stable symmetric nonlinear guided wave solution in region (VI) loses it stability as one crosses the curve into region (IV). On the other hand, keeping the power η_0 and guide width d fixed, we can move vertically by increasing the linear refractive-index mismatch Δ. At $\eta_0 d=1.0$ the unstable symmetric guided wave regains stability as one crosses from region (IV) into region (I). These features were confirmed numerically and are consistent with exactly computed nonlinear guided-wave bifurcation diagrams. In fact, all of the essential features of these bifurcation diagrams including the existence and stability of the nonlinear waves on the surface polariton branch are evident from the potentials sketched for each regime in the figure. Consistent with the single-interface case, we expect that corrections of those potentials in regions (III) and (V) having corners will lead to a smoothing of the latter into local minima. We also observed that when $\eta_0 d \gg 1$, U_s indeed looks like "patched" potentials of the single-interface problem.

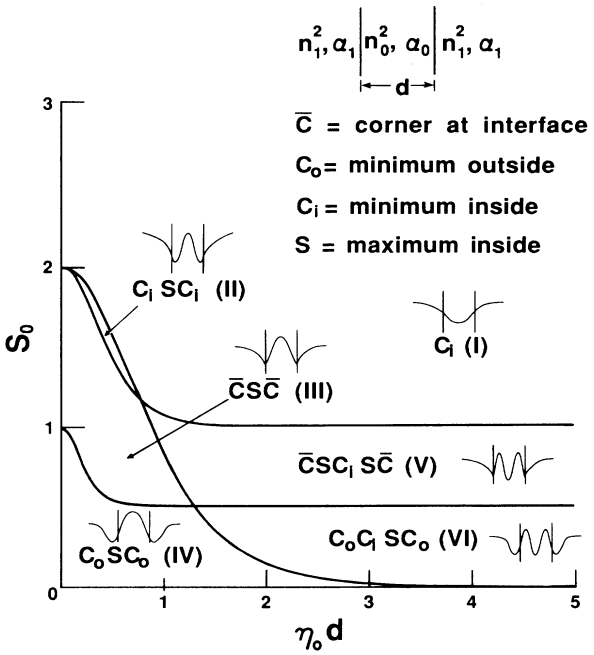

FIG. 7. $S_0,\eta_0 d$ parameter representation of the different potentials in a symmetric waveguide. Here $\alpha=0.5$. Six different regimes are obtained and each is characterized by the critical points of the equivalent potential. In our notation $C_{i(0)}$ means that there is a minimum between (outside the interfaces), **S** means that there is a maximum at $\bar{x}=0$, and $\bar{C}$ means that there is a corner at the interface.

IV. APPLICATIONS: A SOLITON SWITCH AND DIRECTIONAL COUPLER

In this section we are going to show two applications of the theory: a switch based on soliton collision and a directional coupler which relies on a linearly ramped refractive index. In both cases, what we will do in effect is to destabilize stable stationary wave packets propagating close to one interface, by making it collide with a second wave packet.

It is well known that in NLS, solitons have the remarkable property that when two of them with different amplitudes η_i and velocities v_i, $i=1,2$ collide they remain unchanged and each will continue propagating with the same velocity v_i. The net effect of the collision is that the center of mass $\bar{x}_i$ of each is displaced by an amount $\delta\bar{x}_i$, $i=1,2$ where

$$\delta\bar{x}_1 = \frac{v_1-v_2}{|v_1-v_2|4\eta_1}\ln\left[\frac{(\eta_1+\eta_2)^2+\frac{1}{4}(v_1-v_2^2)}{(\eta_1-\eta_2)^2+\frac{1}{4}(v_1-v_2)^2}\right] \tag{9}$$

and $\delta\bar{x}_2=-(\eta_1/\eta_2)\delta\bar{x}_1$. Observe that the sign of $\delta\bar{x}_1$ is the same as that of the relative velocities. Since we will

consider collisions between wave packets with relative velocities, such that the collision time is small, we will approximate its effect by ignoring the perturbation terms due to the interfaces; thus the wave packets will suffer a displacement that will be given by (9). Therefore, if a small moving wave packet collides with a stationary large one, i.e., $\eta_2 < \eta_1$, $v_1 - v_2 = -v_2 < 0$, the phase shift experienced by the larger packet is negative, and the amount of this shift depends on v_2. These assumptions were tested using waveguides whose parameters are that of Figs. 3 and 4. In all cases studied, the stationary wave packet before the collision propagates parallel and to the right of the second interface (see Fig. 5). Its evolution after the collision is obtained by first calculating, using (9), its phase shift due to the collision; the equivalent particle is thus displaced to the left by the computed amount. By ignoring other effects during and after the collision, the subsequent dynamics of the equivalent particle will be determined from its new location. Consider, for example, the case corresponding to Fig. 3, where there are three possibilities of subsequent behavior. First, the displacement is sufficiently large so that the equivalent particle originally located at the bottom of the well to the right of the second interface, is displaced to the left of the nearby maximum and its subsequent dynamics consists of oscillations in the deep potential well between interfaces 1 and 2. The whole trajectory follows *ABCD* in Fig. 3. A numerical solution of (1) shows the corresponding evolution of the wave packet in Fig. 8. The other two possibilities occur if the displacement leaves the particle between the maximum and its original position. In these cases, either the new potential energy of the particle is sufficient to carry it past the new maximum to its right [trajectories $AB'C'D'$ in Fig. 3(b) and $AB''C''C'''D'''E'''$ in Fig. 3(b)], or if it is not large, it will simply oscillate about its original equilibrium position [$AB''C''D''B''$ in Fig. 3(b)]. As in the previous case, the corresponding evolution of the wave packets was obtained from direct integration of the governing equation (1), and we show the results in Figs. 8 and 9. Note that, in some cases, there can be

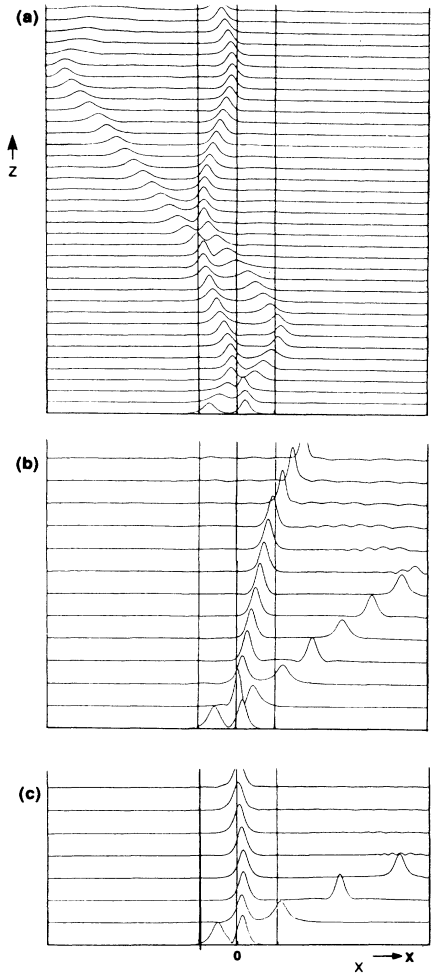

FIG. 8. Evolution of two wave packets in a nonlinear waveguide with the parameters of Fig. 3. The equivalent potential of that figure corresponds to the bigger wave packet. The three cases correspond, respectively, to the three trajectories shown in Fig. 3(b). The power of the bigger packet is $P = 2.0$ and that of the smaller is $P = 1.2$.

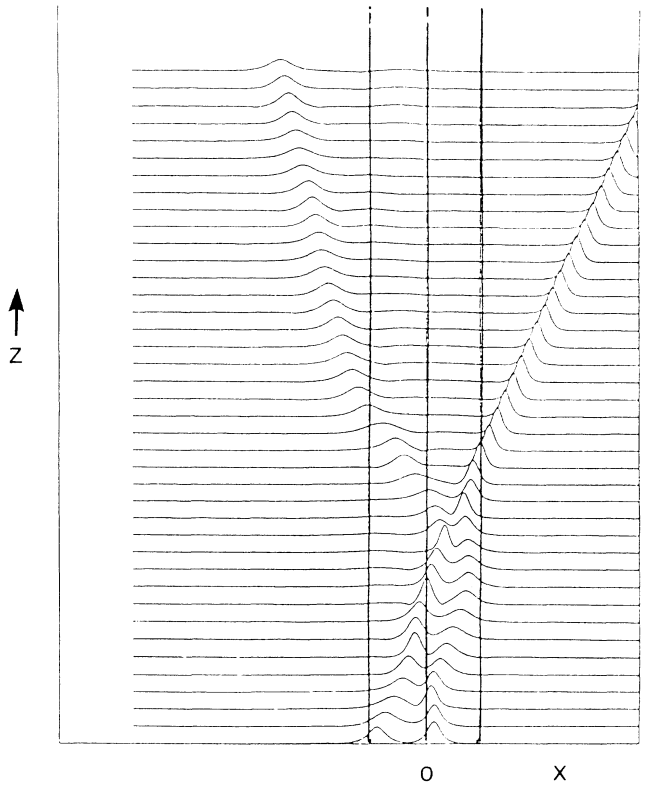

FIG. 9. Evolution of two wave packets in a nonlinear waveguide with the parameters of Fig. 4. The equivalent potential of that figure corresponds to the bigger wave packet. Here, the packet originally propagating parallel to the second interface with power $P = 1.6$ evolves according to the theoretical trajectory shown in Fig. 4(b). For the incident wave packet $P = 1.2$ and $v_0 = 0.36$.

more than one collision between the two wave packets and each collision changes the trajectory according to (9). Although our main focus has been the evolution of the originally stationary wave packet, one can also describe the small incident wave packet. Figure 10 shows the potential and phase portrait of its equivalent particle, where the theoretical trajectory *abcdef* contains all the features of the actual evolution seen on Fig. 9. We can think of this effect as that of a scanner where the parameters of the second wave packet determines the asymptotic location of the first one.

Looking back to the case shown in Fig. 9, where the wave packet that originally was propagating near the second interface ends up in the far right, if in the medium next to the third interface, we add a suitable x dependence on the linear refractive index, we can design a switch.

It is known that if there are no interfaces but instead the refractive index of the dielectric n^2 has the form $n_1^2+\alpha_1|F|^2-\gamma x$, then

$$A(x,\tau)=\sqrt{\alpha_1/2}F(x,z)e^{i(\beta^2-n_1^2)z/(2\beta)}$$

will satisfy

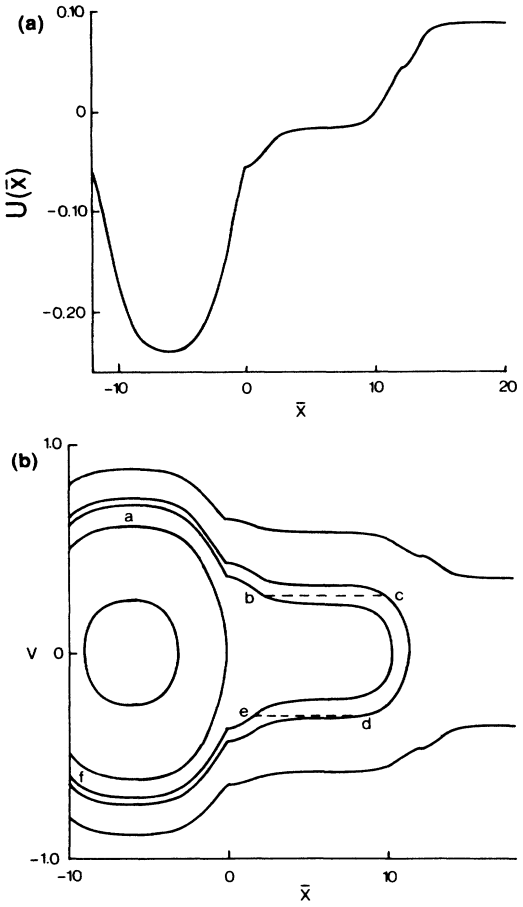

FIG. 10. Potential and phase plane of the equivalent particle corresponding to the smaller wave packet of Fig. 9. Again, in the phase plane we show the theoretical trajectory of the equivalent particle.

$$\frac{\partial A}{\partial \tau}-i\frac{\partial^2 A}{\partial x^2}-2i|A|^2A=-2i\gamma x A \ .$$

Using perturbation theory as we did earlier in I to obtain the equivalent-particle description for beams, or by calculating the solution exactly,[10] one finds that A has the soliton shape where now

$$\frac{d\bar{x}}{d\tau}=v, \quad \frac{dv}{d\tau}=-4\gamma \ ,$$

that is, the equivalent particle experiences a deceleration of 4γ.

Having introduced this new behavior, the designing of the switch becomes very simple. We now assume for the case shown in Fig. 9 that the dielectric at the right of the third interface has a refractive index that starts decreasing by γx after some x' to the right of the location of the minima in the equivalent potential. Then, the equivalent particle, once it crosses x', will start decelerating and with the proper choice of parameters, the idea is to eventually have the particle oscillating about the well next to the third interface. We achieved this by choosing x' to be one unit distance from the location of the minima and $\gamma=0.05$ (see Fig. 11). The whole experiment describes a switch of a wave packet initially propagating parallel to the second interface, to a new trajectory parallel to the third interface. The switching mechanism was triggered by a second wave packet.

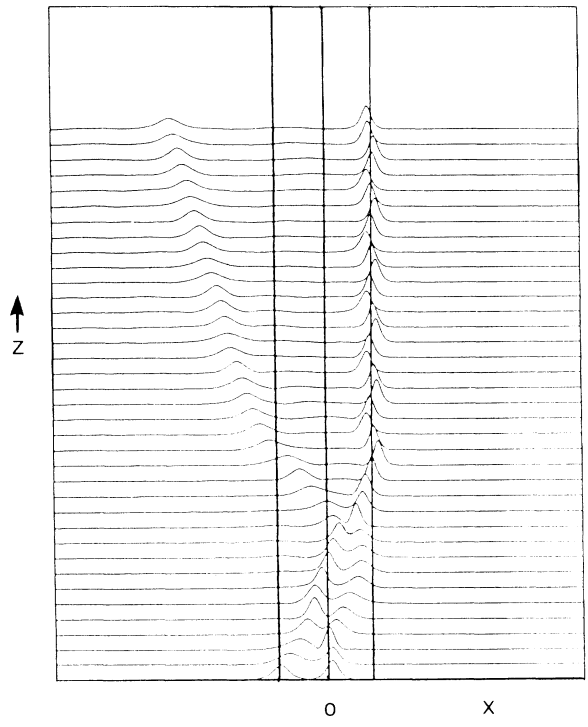

FIG. 11. Trapping of the wave packet originally propagating parallel to the second interface located at $x=0$. For $x>13.8$, the linear refractive-index coefficient decreases linearly in x. The constant of proportionality γ is 0.05. The parameters of the media are those of Fig. 4, and of the wave packets, are those of Fig. 9.

V. BOUND SOLITONS

For most of this work, we have considered initial wave packets that have the sech-like shape typical of the one-soliton solution of NLS. However, interesting phenomena can occur for different initial conditions. As stated earlier, if initially the wave packet is of arbitrary shape and far away from an interface, it will decompose into its soliton and radiation components, and if each soliton has different velocity, they will eventually separate before reaching the interface and evolve as individual wave packets. After that, the dynamics of each component is determined by its own potential, as we have just shown. Possible collisions between wave packets can now be understood in the context of the equivalent-particle dynamics. If, instead, our initial wave packet is a bound-N soliton state, that is, N soliton components each with the same parameter v, the dynamics is more complicated since the nonlinear interaction between solitons, so far ignored in the analysis, is essential for this case. We present here some numerical simulations for the simplest case of a bound two-soliton initial condition[11] as it approaches an interface.

In the absence of an interface, the soliton components interact in a periodic fashion, as we can see in Fig. 12. There the two solitons, each with different η, oscillate about the center of mass which moves with velocity v. We now put in the interface. Since each soliton component has a different η, we can expect that the effect of the interface is different for each one (one has to remember that in the single-soliton dynamics the equivalent potential was η dependent). The question is whether this different effect is enough to cause the solitons to split. Two cases are shown in Figs. 13 and 14; both cases have the same parameters except for the velocity of the center of mass, which is bigger in Fig. 14. Indeed, we see splitting occurring at the interface in both cases, and in the second case we see that one of the components seems to be trapped near the corresponding minimum of its equivalent potential.

To understand the dynamics with an equivalent two-particle description, we follow the same approach used in Sec. IV of paper I and, using the conservation laws, obtain a nonlinear system of equations for the soliton parameters $v_i \eta_i$. The first is $(d/d\tau)(\eta_1+\eta_2)=0$. Alternatively, one can use the perturbation theory on the scattering data of the linear problem associated with NLS (A1).[12] A set of four equations, one for each parameter is obtained. The first two are $d\eta_i/d\tau=0$, $i=1,2$ and the last two

$$\frac{dv_i}{d\tau} = -\int_{-\infty}^{\infty} V(A\psi_{2i}^2 - A^*\psi_{1i}^2)dx, \quad i=1,2$$

where ψ_{ni}, $n=1,2$ are the eigenfunctions of (A1) when $A(x,0)$ in the exact two-soliton solution of NLS.[11]

In contrast with the one-soliton case, we cannot solve these equations analytically; one would have to do it numerically. This approach was used by Kodama and Nozaki in Ref. 13, to describe soliton splitting in an optical fiber. We are not going to do it for this case here; in-

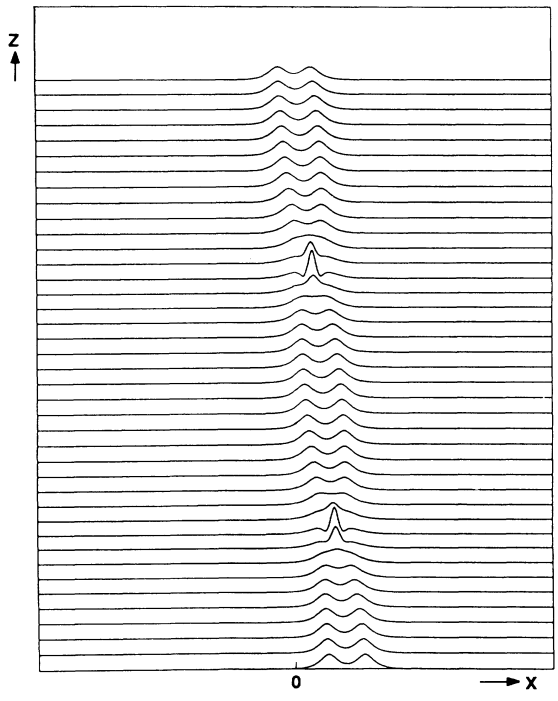

FIG. 12. Evolution of an initial bound two-soliton wave packet in a nonlinear medium with no interface. The soliton parameters are $\eta_1=0.35$, $\eta_2=0.25$ and the center of mass velocity is -0.2.

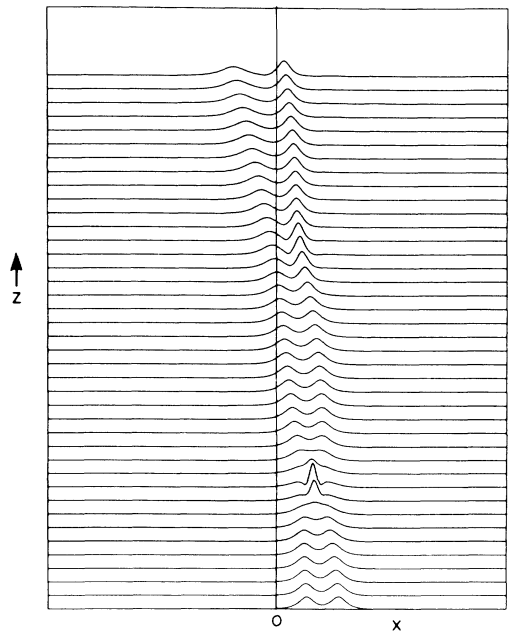

FIG. 13. Evolution of an initial bound two-soliton wave packet with parameters as in Fig. 12 approaching an interface. Splitting is observed, with one soliton staying in the right-hand medium. Here, $\Delta=0.1$ and $\alpha=0.75$.

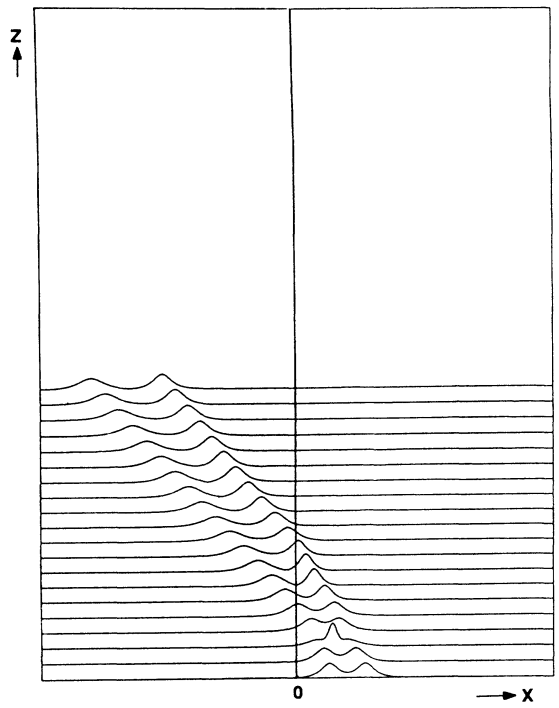

FIG. 14. Evolution of an initial bound two-soliton wave packet approaching an interface. Here, the velocity of the center of mass is now -0.3, bigger than in the previous figure. Even though splitting still occurs, both packets cross the interface.

stead, we will only say that once they are separated the propagation of each component can be described from its equivalent potential.

VI. CONCLUSIONS

In this second paper of the series we have illustrated how concepts well known in soliton theory can be extended in a straightforward fashion to study a variety of problems which would otherwise be intractable if one had to rely solely on full-scale numerical simulation. The resistance of spatial solitons, which are the mathematical realization of self-focused light channels in the present context, to perturbations or collisions with other solitons, makes a classical particle description possible. In effect, the small amount of radiation generated due to interaction with the interface acts as a weak dissipation in an otherwise conservative problem. The results illustrate how global inferences can be drawn about the trajectory of a self-focused channel as it encounters one or more optical interfaces. If it should break into multiple channels, the number created and amount of radiation generated is known *a priori*, without recourse to numerical study. Whether it stays as a single entity or breaks up after crossing an interface, the channels trajectory (or those of its components in the event of breakup) can be traced accurately. Its subsequent behavior due to interaction with another interface or collision with another component (usually reflected) can also be predicted. In all cases we have confirmed the validity of the theory with extensive numerical computation.

The question of the stability of the nonlinear surface and guided waves is very important from a physical standpoint. If a nonlinear surface or guided wave is unstable then any experimental attempts to couple light into it will fail. Stability analysis of these waves is very complicated, requiring consideration of the stability of global orbits in phase space rather than fixed points in more conventional cases. With the exception of the analytic stability result presented here, there exists only two analytic stability predictions for nonlinear waveguides.[6,7] The earliest prediction relied on a topological argument[6] while the later one combines this with a variational approach.[7] Our results for the thin-film waveguide in Sec. III confirm these stability predictions and, moreover, provide a very natural global picture in terms of particles in potentials and their equilibria. The main inference to be drawn from our work in both papers is that the restricted concept of stationary nonlinear surface or guided waves is too limited and is of little use in analyzing or understanding the nonlinear behavior of propagating optical beams in multi-layered structures.

ACKNOWLEDGMENTS

This work was carried out under the auspices of the Arizona Center for Mathematical Sciences, which is funded by U.S. Air Force Grant No. AFOSR: F49620-86-C0130. One of the authors (J.V.M.) would like to acknowledge partial support from the United Kingdom Science Research Council, Grant No. GR/D/84726.

APPENDIX

It is well known that for the NLS equation there is an associated linear eigenvalue problem, first obtained by Zakharov and Shabat,[11] which determines from the scattering data, the soliton and radiation components of a given initial condition $A(x,0)$. The associated linear problem is

$$\begin{aligned} i\frac{\partial\psi_1}{\partial x}+A(x,0)\psi_2=\varsigma\psi_1\ , \\ -\frac{\partial\psi_2}{\partial x}+A^*(x,0)\psi_1=\varsigma\psi_2\ , \end{aligned} \tag{A1}$$

and Satsuma and Yajima[2] obtained the scattering data of (A1) for the class of potentials

$$A(x,0)=A(\mathrm{sech}x)e^{ivx/2}\ .$$

They found that there are N discrete eigenvalues of (A1) $\varsigma_n=-v/4+i(A-n+\frac{1}{2})$, $n=1,\ldots,N$, where $A-\frac{1}{2}<N\leq A+\frac{1}{2}$ and there is also some continuous spectrum. For NLS this means that the outcome of this initial condition is a bound N-soliton component plus a radiation component. The bound state propagates with velocity v and in the evolution it shows periodic behavior as in Fig. 12. We now relate this result to our problem. The question that was left open in Sec. IV of paper I was,

what happens to a wave packet when it crosses the interface? We already explained in Sec. IV of I that in the nonlinear regime, which is the case of interest here, the wave packet suffers no initial changes as it crosses the interface. However, once it has crossed, it will no longer be a perfect soliton of the new medium and it will consequently decompose into the normal modes associated with the new medium. The way we will find these new modes is by solving the corresponding linear eigenvalue equivalent to (A1) for the nonlinear Schrödinger-like equation in the right-hand medium, where the potential in the linear problem will be the incoming wave packet. The result will be, after a proper scaling, similar to the one shown above.

Suppose that one has an initial condition for the field in the right-hand medium where the nonlinear refractive index is α_1 a "natural" soliton of the left-hand medium given by

$$F(x)=\sqrt{2/\alpha_0}\,2\eta_0\,\mathrm{sech}[2\eta_0(x-\bar{x})]e^{i(vx/2+2\sigma)} . \tag{A2}$$

If, as we did in Sec. IV of I, we define the field to be

$$F(x,z)=\sqrt{2/\alpha_1}\,A(x,\tau)e^{i(\beta^2-n_1^2)\tau} ,$$

then $A(x,\tau)$ satisfies for the right-hand medium the exact NLS, and from (A2) its initial condition would be

$$\frac{1}{\sqrt{\alpha}}2\eta_0\,\mathrm{sech}[2\eta_0(x-\bar{x})]e^{i(vx/2+2\sigma_0)} . \tag{A3}$$

Now the question of finding the normal-mode decomposition of a "natural" soliton of the left-hand medium in the right-hand medium translates into find the scattering data of (A1), with Eq. (A3) as potential. But this is now a simple problem, since if we make the following transformations,

$$x'=2\eta_0(x-\bar{x}) ,$$
$$\psi_1'=\psi_1 e^{-i[v(\bar{x}/2)+2\sigma_0]} ,$$
$$\psi_2'=\psi_2 e^{i[v(\bar{x}/2)+2\sigma_0]} ,$$

(A1) becomes

$$\begin{aligned} &i\frac{\partial\psi_1'}{\partial x'}+A'(x')\psi_2'=\varsigma'\psi_1' ,\\ &-i\frac{\partial\psi_2'}{\partial x'}+A'^{*}(x')\psi_1'-\varsigma'\psi_2' , \end{aligned} \tag{A4}$$

where now

$A'(x')=1/\sqrt{\alpha}(\mathrm{sech}x')e^{ivx'/2\eta_0}$ and $\varsigma'=\varsigma/2\eta_0$. This is exactly the case mentioned at the beginning of this section, and if we translate the result shown above to this particular problem one has that (4) will decompose into N solitons and radiation where now $1/\sqrt{\alpha}-\frac{1}{2}<N\le 1/\sqrt{\alpha}$. Each soliton has parameters $\varsigma_n=-v_n/4+i\eta_n=-v/4+i(1/\sqrt{\alpha}-n+\frac{1}{2})2\eta_0$, $n=1,\ldots,N$. Observe that since $\alpha=\alpha_0/\alpha_1\le 1$, $N\ge 1$.

We can also quantify the amount of power transferred into radiation modes using the trace formulas which are the nonlinear analogue of the Parseval's relations.[10] These formulas relate the conserved quantities of NLS, C_n, with the scattering data of (A1) and they are

$$C_n=2i\sum_{k=1}^{N}\frac{\varsigma_k^n-\varsigma_k^{*n}}{n}+\frac{1}{\pi}\int_{-\infty}^{\infty}\varsigma^{n-1}\ln(1-|R|^2)d\varsigma ,$$

where ς_k are the discrete eigenvalues of (A1) and R is the reflection coefficient given in terms of the continuous spectrum of (A1). For $n=1$ one has $C_1=-\int_{-\infty}^{\infty}AA^{*}dx$; therefore

$$-C_1=4\sum_{k=1}^{N}\eta_k-\frac{1}{\pi}\int_{-\infty}^{\infty}\ln(1-|R|^2)d\varsigma . \tag{A5}$$

If $A(x,0)$ is an almost reflectionless potential, which, as we will see, is the case in our problem, $|R|\ll 1$, and in this case the amount of power in the radiation modes given by the integral of $|R|^2$ simply is

$$\int_{-\infty}^{\infty}|R|^2d\varsigma=\pi\int_{-\infty}^{\infty}AA^{*}dx-4\pi\sum_{k=1}^{N}\eta_k . \tag{A6}$$

If instead one has the case of a soliton initially in the right-hand medium and crossing the interface, to determine the decomposition of this soliton in the new medium, one can proceed as before to find that, for this case, the number of soliton components is $\sqrt{\alpha}-\frac{1}{2}<N\le\sqrt{\alpha}+\frac{1}{2}$. Therefore, if $0<\alpha<0.25$ the field in the left-hand medium will contain no soliton components and (A6) is for this case Parseval's identity. If $0.25\le\alpha\le 1$, a single soliton will prevail but with new parameters $\varsigma_1=-v/4+(\alpha-\frac{1}{2})2\eta_1$ and radiation, with the powers carried by each part given by (A3). The interpretation of these results in terms of the original wave packets and the subsequent dynamics of each new component is explained in Sec. II of this paper.

*Permanent address: Physics Department, Heriot-Watt University, Riccarton, Edinburgh EH14 4AS, Scotland.

[1]A. B. Aceves, J. V. Moloney, and A. C. Newell, Phys. Rev. A **39**, 1809 (1989).

[2]J. Satsuma and N. Yajima, Prog. Theor. Phys. Suppl. **55**, 284 (1974).

[3]P. W. Smith and W. J. Tomlinson, IEEE J. Quantum Electron. **QE-20**, 30 (1984).

[4]W. J. Tomlinson, J. P. Gordon, P. W. Smith, and A. E. Kaplan, Appl. Opt. **21**, 2041 (1982).

[5]N. N. Akhmediev, Zh. Eksp. Teor. Fiz. **83**, 545 (1982) [Sov. Phys.—JETP **56**, 299 (1982)]; C. T. Seaton, J. D. Valera, R. L. Shoemaker, G. I. Stegeman, J. T. Chilwell, and S. D. Smith, IEEE J. Quantum Electron. **QE-21**, 774 (1985).

[6]C. K. Jones and J. V. Moloney, Phys. Lett. **117A**, 175 (1986).

[7]M. Grillakis, J. Shatah, and W. Strauss, J. Funct. Anal. (to be published).

[8]A. Yariv, *Optical Electronics* (Holt-Saunders, New York, 1985).

[9]J. V. Moloney, J. Ariyasu, C. T. Seaton, and G. I. Stegeman, Appl. Phys. Lett. **48**, 826 (1986); L. Leine, Ch. Wachter, U. Langbein, and F. Lederer, Opt. Lett. **11**, 590 (1986).

[10]D. J. Kaup and A. C. Newell, Proc. R. Soc. London, Ser. A **361**, 413 (1978).

[11]V. E. Zakharov and A. B. v. Shabat, Zh. Eksp. Teor. Fiz. **61**, 118 (1971) [Sov. Phys.—JETP, **34**, 62 (1972)].

[12]A. C. Newell, *Solitons in Mathematics and Physics, Conference Board of Mathematical Sciences—National Science Foundation* (SIAM, Philadelphia, 1985).

[13]Y. Kodama and K. Nozaki (unpublished).